AUTHOR(S): MALEVU, T.D., OCAYA, R.O., TSHABALALA, K.G. and FERNANDEZ, C.

TITLE: Synthesis and characterization of high-quality PbI 2 nanopowders from depleted SLA accumulator anode and cathode.

YEAR: 2016

Publisher citation: MALEVU, T.D., OCAYA, R.O., TSHABALALA, K.G. and FERNANDEZ, C. 2016. Synthesis and characterization of high-quality PbI 2 nanopowders from depleted SLA accumulator anode and cathode. Applied physics A [online], 122(7), article 630. Available from: https://dx.doi.org/10.1007/s00339-016-0158-9

OpenAIR citation: MALEVU, T.D., OCAYA, R.O., TSHABALALA, K.G. and FERNANDEZ, C. 2016. Synthesis and characterization of high-quality PbI 2 nanopowders from depleted SLA accumulator anode and cathode. Applied physics A, 122(7), article 630. Held on OpenAIR [online]. Available from: https://openair.rgu.ac.uk

Synthesis and characterization of high quality PbI_2 nanopowders from depleted SLA accumulator anode and cathodes

Department of Physics, University of the Free State, P. Bag X13, Phuthaditjhaba 9866.
Email: malevutd@ufs.ac.za

Abstract

High quality lead iodide (PbI_2) nanoparticles were synthesized from both anode and cathode of a discarded sealed lead-acid accumulator as starting materials. The structure, morphology, chemical composition and optical properties of washed PbI_2 were investigated using XRD, SEM, PL and EDS. The XRD measurements indicated the presence of pure hexagonal PbI_2 nanoparticles. Application of the Scherrer equation indicates crystal sizes between 13.703 and 14.320 nm. SEM indicated the presence of spherical particle agglomerations between 1.5 and 3.5 μm in diameter. The measured band gap using two methods was consistent at 2.75 eV. EDS results suggest the absence of impurities in the synthesized nanoparticles. The overall results suggest that discarded sealed lead-acid accumulators can source pure hexagonal phase lead iodide nanoparticles with potential applications in perovskite solar cells.

Keywords: Lead iodide nanopowders, SLA battery, perovskite solar cell

1. Introduction

PbI_2 is a lamellar semiconducting solid comprising lead and iodide ion layers in covalent bonding. Weak van der Waals interactions hold these layers together in a three-dimensional hexagonal close-packed (hcp) array of iodide anions with alternate layers of octahedral lattices with lead (II) cations interstitially sited. Figure1 shows the layered crystal structure of PbI_2.

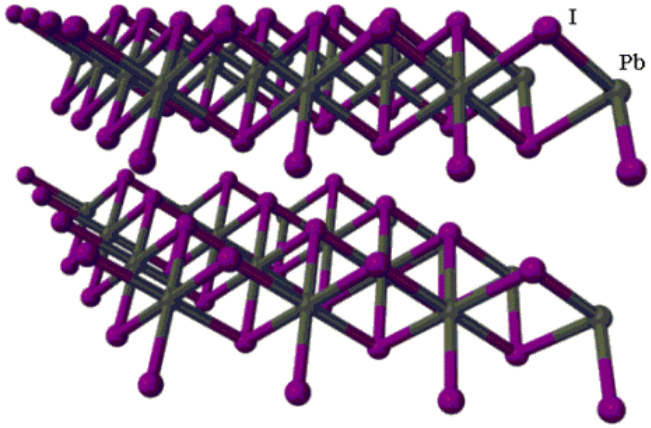

Figure 1: Layered structure of PbI_2 [1]

The lattice consists of a repeating I-Pb-I sequence [2] with high atomic number ($Z_{Pb} = 82$, $Z_I = 53$) and intrinsic band gap of about 2.4 eV. These properties make it a potential candidate for room-temperature, direct detectors of low energy ionizing x- and γ- rays [3]. There is growing interest in the use of this material in lead-based perovoskite solar cells. The economical application to solar cells depends highly on the ease of fabrication and growth processes and on the purity and yield of PbI_2 [4]. It is generally believed that the properties of PbI_2 depend not only on their chemical purity, but

also on precise chemical structure, phase, morphological distribution and dimensionality. A challenging issue presently faced in materials synthesis is the problem of controlling the mesoscopic anisotropy in inorganic materials. Extensive studies of the influence of purity of precursor PbI_2 powders on single bulk crystal growth have reported varying degrees of success in the literature [5]. Examples of currently used methods that yield micro- or nano-PbI_2 structures are low temperature colloidal process [6], reverse micelles method [7], vapor-transporting method [8], hydrothermal [9] and vapor deposition [2]. The hydrothermal method is considered the method of choice to prepare the bulk nanoparticle semiconductor with well-controlled morphologies at lower temperature using a one-step procedure [10]. In this work, PbI_2 nanoparticle bulk has been synthesized from both the anode and the cathode of a discarded lead-acid accumulator cell. This route is potentially economically viable from the perspective of both source material and processing costs. Lead is a well-known environmental hazard and its safe disposal presents a perpetual challenge in the light of its abundance in high-density energy electrochemical storage devices. The lead in depleted accumulators is currently destined mostly for recycle and reuse in similar accumulators. In this paper the suggested reuse of such lead sources in lead perovskite solar cells opens up interesting future possibilities for more experimentation and development. In aid of this, the present paper reports on investigations of synthesis, optical, structural, morphological characterizations and purity assessments of PbI_2 for solar cell applications.

2. Experimental

Metallic lead (Pb) anode and lead dioxide (PbO_2) cathode material were extracted from one cell of a depleted sealed-lead acid gell (SLAG) battery. The un-purified yield Pb and PbO_2 were 66.8 g and 89.0 g respectively. Two routes were taken to synthesize PbI_2. The first used the anode and the second the cathode.

2.1. Synthesis of PbI_2 using anode

The anode material was soaked in hot water for 1 hr three times to remove the combining gel from the surface. Immediately after washing, the metallic lead was oven dried for 1 hr at 80 ^{o}C and allowed to cool to room temperature. The metallic lead was then broken up into small pieces and placed in a 500 mL glass beaker. The glass beaker was placed on a hot plate and 40 mL of concentrated nitric acid (55%) was poured into the beaker and allowed to boil under gentle magnetic stirring. When no further reaction of lead and acid was visible, 20 mL of deionized was added to create a dilute solution and the precipitate was decanted and collected. The un-reacted metallic was subjected to the same procedure until no further lead remained. The process was repeated 3 times resulting in 4 white $Pb(NO_2)_2$ samples in four different beakers. A solution of potassium iodide (KI) was prepared by dissolving 10 g of potassium iodide powder in 50 mL of deionized water. The KI was added into $Pb(NO_2\ )_2$, giving yellow PbI_2 solution. Eq.1 and Eq.2 describe the two synthesis routes. The solution was then washed with deionized water and dried at 300 ^{o}C for 1 hr resulting in a yellow, dry PbI_2 powder. The samples were then allowed to cool naturally to room temperature prior to

characterization.

$$3\ \mathrm{Pb} + 8\ \mathrm{HNO_3} \rightarrow 3\ \mathrm{Pb(NO_3)_2} + 2\ \mathrm{NO} + 4\ \mathrm{H_2O} \tag{1}$$

$$\mathrm{Pb(NO_3)_2} + 2\mathrm{KI} \rightarrow 2\mathrm{KNO_3} + \mathrm{PbI_2} \tag{2}$$

2.2. Synthesis of PbI_2 using cathode

PbI_2 may also be synthesized using the cathode precursor and acetic acid according to the equation:

$$\mathrm{PbO} + 2\ \mathrm{CH_3COOH} \rightarrow \mathrm{Pb(CH_3COO)_2} + \mathrm{H_2O} \tag{3}$$

$$\mathrm{Pb(CH_3COO)_2} + 2\ \mathrm{KI} \rightarrow \mathrm{PbI_2} + 2\ \mathrm{CH_3COOK} \tag{4}$$

The as-collected lead dioxide (PbO_2) was washed with deionized and oven dried for 1 hr at 80 ^{o}C. After drying, 34.66 g of (PbO_2) was annealed at 600 ^{o}C for 5 hrs resulting in lead oxide (PbO). The obtained PbO was mixed in 50 mL of acetic acid in a glass beaker. The solution was brought to the boil on a hot while magnetically stirring. The precipitate of $Pb(Ch_3COO)_2$ was collected and dried at 80 ^{o}C for 1 hr and then mixed in a glass beaker with a solution of KI prepared by dissolving 10 g of potassium iodide powder in 50 mL of deionized water. The solution was heated until the liquid completely boiled away. The precipitate was collected and oven dried for 50 mins. The sample was allowed to cool naturally to room temperature resulting in a homogeneous powder for characterization.

3. Characterization

The structure of PbI_2 was determined using X-ray diffraction (XRD, Bruker AXS D8 Advanced) with CuKα 1.5418Å wavelength radiation. Particle morphology and chemical composition of the samples were studied using the Joel JSM-9800F field emission scanning electron microscope (FE-SEM) equipped with an energy dispersive x-ray spectrometer (EDS). PL measurements were done using a Carry Eclipse fluorescence spectrophotometer equipped with a 150W xenon (Xe) lamp as excitation source at an wavelength of 220 nm.

4. Results and Discussion

4.1. Structural analysis

To understand the formation and evolution of PbI_2 phase and crystallization, XRD measurements of the PbI_2 powders were carried out. Figure 2 shows the XRD patterns of PbI_2 for four different washing processes labeled (PbI_1-1 to PbI_2-4). The 2θ diffraction peaks occur at 22.45^o, 25.94^o, 34.18^o, 38.56^o, 39.73^o, 41.72^o, 45.31^o, 47.85^o, 52.41^o, 53.28^o, 56.53^o, 61.61^o, 63.71^o, 67.65^o, and 68.44^o. These peaks respectively correspond exactly to crystal plane reflections (100), (011), (102), (003), (110), (111), (103), (200), (022), (113), (023), (114), (212) and (300). These reflections correspond to the standard card (JCPDS:80-1000) of hexagonal PbI_2 structure. This suggests the absence of impurities in the powder PbI_2 products.

The evolution of Figure 2 further suggests that with more sample washing and re-heating the diffraction peaks become narrower with higher intensity. Further evidence of this can be seen in Figure 3, which is a detailing of

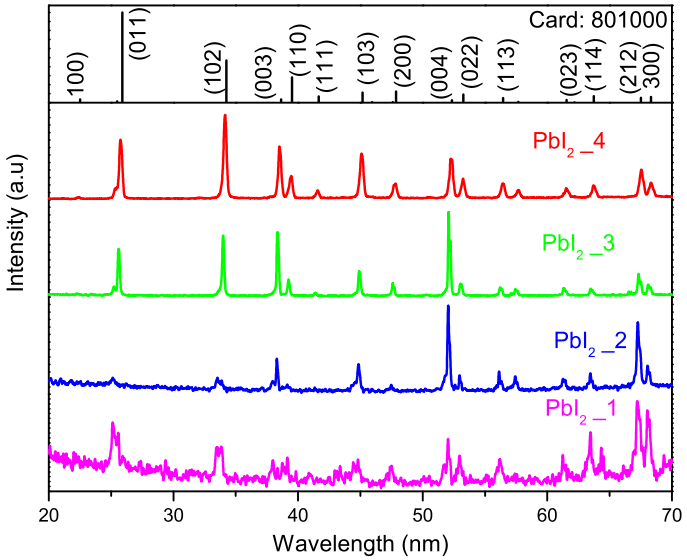

Figure 2: XRD patterns of PbI_2 at different washing and synthesis method

the XRD pattern at the (102) reflection. The observations suggest pure and highly crystalline PbI_2 structure is attainable by washing. The mean crystallite particle size was estimated using the Debye-Scherrer equation [11, 12].

$$\mathrm{D} = \frac{k\lambda}{\beta \cos\theta} \tag{5}$$

where D is the size of the crystallites, β is the full-width at half-maximum (FWHM) of a diffraction line located at angle θ, λ is the x-ray wavelength and k=0.9 is the Scherrer constant, which depends on the peak breadth, crystallite shape, and crystallite size distribution. Five prominent peaks for all samples were chosen to estimate the average crystallite size of PbI_2 nanostructures by the least squares method. The estimated crystallite sizes are 13.703, 11.587, 12.494, and 14.32 nm for samples heated in ascending order. It is evi-

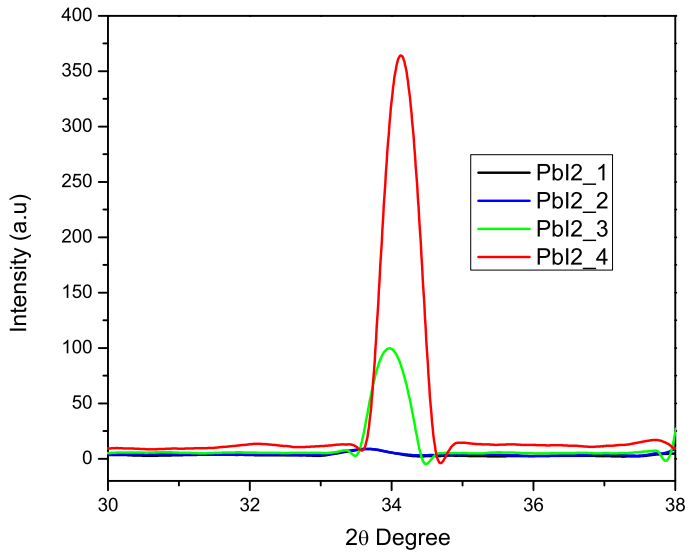

Figure 3: Detailed XRD pattern showing the effect of washing and synthesis method on PbI_2 intensity

dent that the crystallite sizes increase with washing intensity, thus confirming the literature observation that the growth and synthesis method is significant in the fabrication of PbI_2 nanostructures [13]. To further investigate all electrodes as possible sources of lead iodide the acetic acid method was used. Figure 4(a) is the XRD pattern of the cathode-sourced PbO_2 nanoparticles. The figure matches the standard card: (JCPDS:73-0851) with few impurity peaks, which are attributable to unwashed remnant gel sulphuric acid. Figure 4(b) XRD pattern indicates the presence of PbO nanoparticles after annealing PbO_2 particles for 5 hrs. Figure 5 XRD shows the presence of PbI_2 nanoparticles synthesized using the cathode. The figure matches the standard card (JCPDS:80-1000) corresponding to PbI_2 nanoparticles. The mea-

sured 2θ diffraction angles are 22.45^o, 25.94^o, 34.18^o, 38.56^o, 39.73^o, 41.72^o, 45.31^o, 47.85^o, 52.41^o, 53.28^o, 56.53^o, 61.61^o, 63.71^o, 67.65^o, and 68.44^o. The corresponding reflections are (100), (011), (102), (003), (110), (111), (103), (200), (022), (113), (023), (114), (212) and (300) respectively. No impurity peaks were observed.

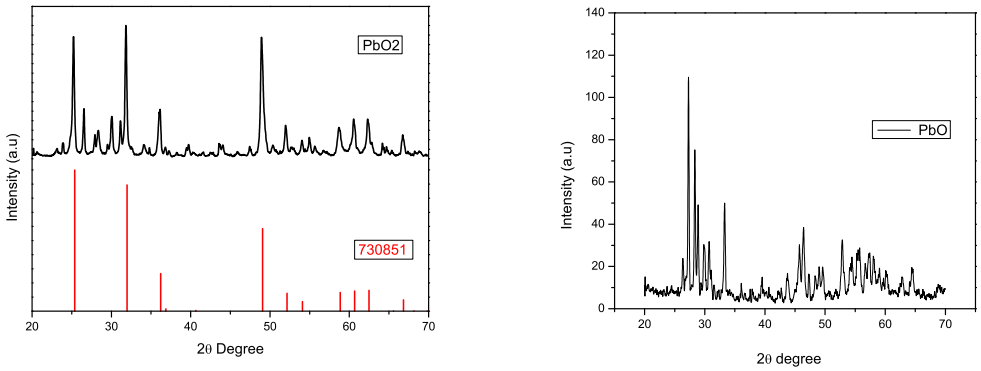

(a) (b)

Figure 4: XRD patterns of (a) PbO_2 extracted from cathode (b) PbO after annealing at 600 ^{o}C.

4.2. Morphology and chemical composition

The morphology, chemical composition and elemental distribution of the samples were investigated by scanning electron microscopy. Figures 6(a)-(e) indicate that for both anode and cathode precursors the PbI_2 particle morphology is approximately spherical with the varying diameters. However, for the anode precursor the resultant particles increase in size with increased washing, as shown in Figures 6(a)-(d). From 6(a) it is clear that the powder consisted of various particles sizes and morphologies making exact size determination more difficult, although average particle size was estimated at

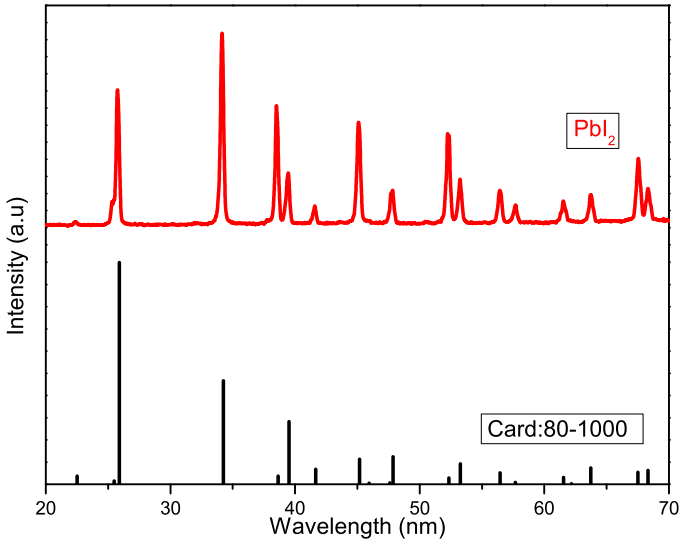

Figure 5: XRD patterns of PbI_2 from cathode

691.60 nm. It is evident from the improved contrast SEM images in Figures 6(b)-(d) that some nanoparticle agglomeration occurred to form larger clusters with diameters averaging 1.87, 3.16 and 3.40 μm respectively. Figure 6(e) shows nanoparticles synthesized from the cathode precursor material, with average particle size at approximately 1.526 μm. Both methods gave similar particle arrangement and general morphology.

Figure 7 shows the SEM elemental mapping measurements of the PbI_2 particles from both anode and cathode starting materials. The figure data suggest the absence of impurities except carbon attributable to post heating, and potassium, which can be attributed to un-reacted precursors. Figure 8 shows the traditional EDS measurements on the PbI_2 products for both anode and cathode starting materials. The results are in agreement with those

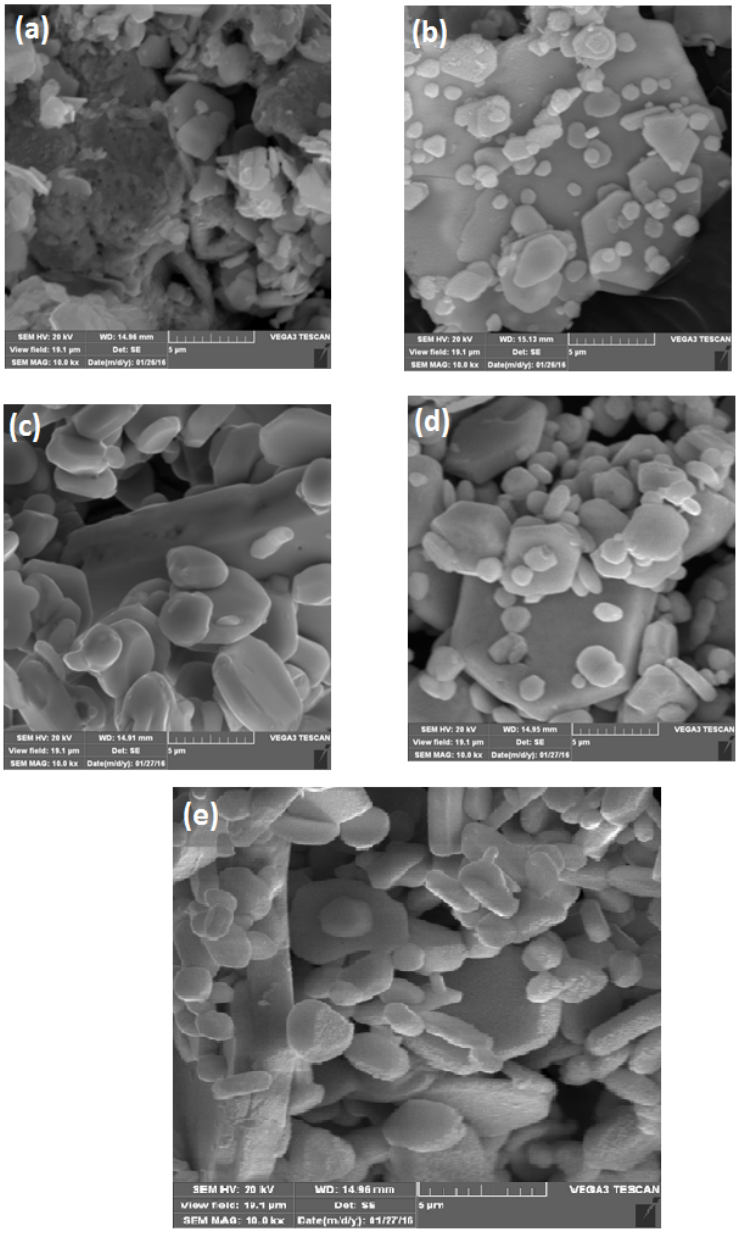

Figure 6: SEM micrographs of PbI_2 from anode (a)-(d) and cathode (e).

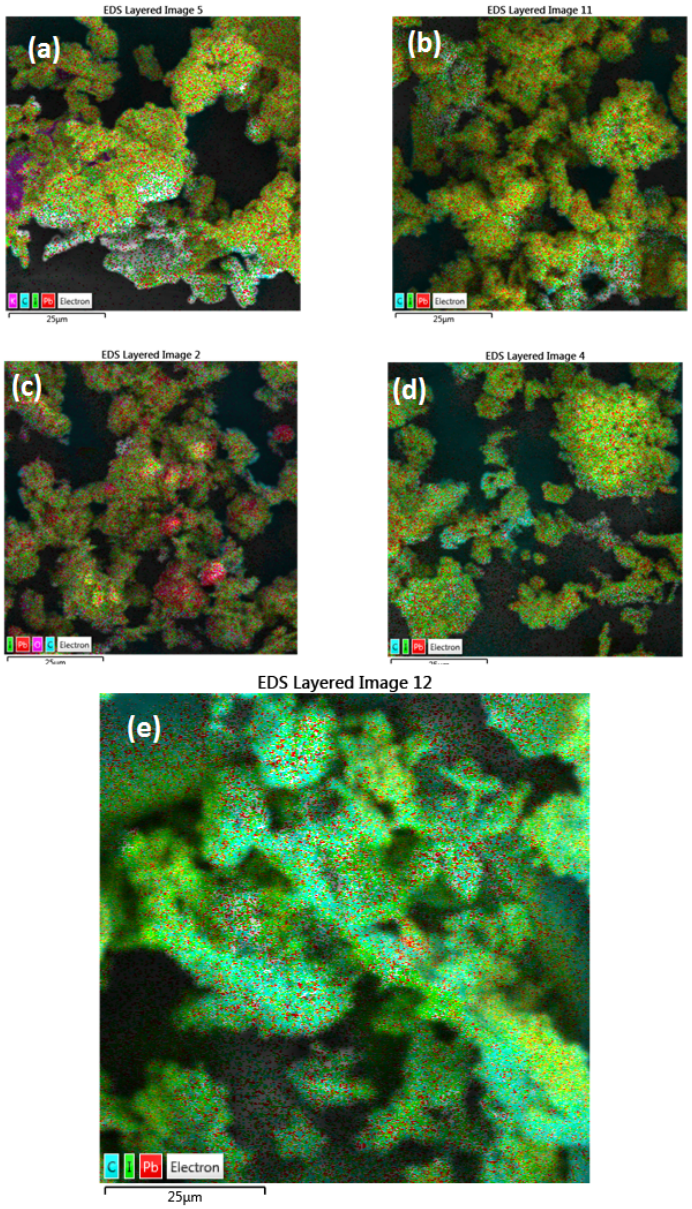

Figure 7: SEM images of PbI_2 elemental mapping from anode (a)-(d) and cathode (e).

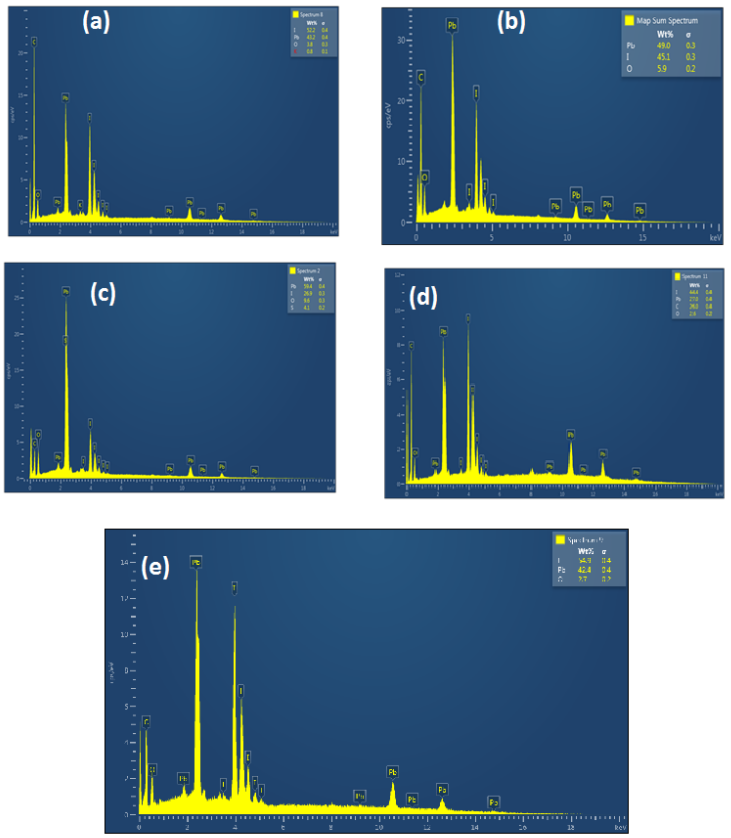

Figure 8: EDS of PbI_2 particles.

from the SEM elemental mapping measurements. However, in spite of the prominent Pb, I, K and C peaks in the EDS spectrum, the weight percentage of Pb, and I elements obtained from EDS is nearly stoichiometric. This is a good indication that both source materials are good starting materials for PbI_2 nanoparticles and may be suitable for further exploration of lead iodide perovskite solar cells.

4.3. Optical properties

PL measurements on anode-sourced PbI_2 nanostructures was carried out using 200 nm wavelength excitation. Figure 9 shows the spectra obtained by monitoring PbI_2 emissions on the blue emission band, between 440 to 500 nm. One broad peak was observed centered at 457 nm. This is attributed to the free excitons [14], [15]. The maximum emission intensity for PbI_2

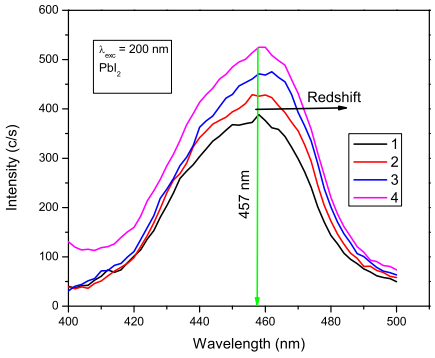

Figure 9: PL emission spectra of anode-sourced PbI_2 (λ=200 nm).

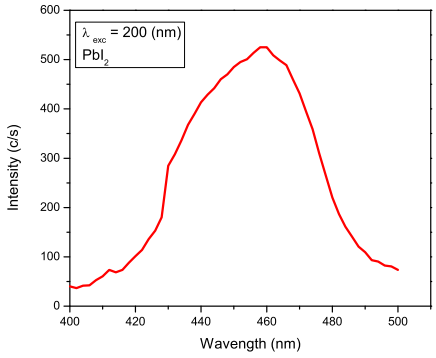

Figure 10: PL emission spectra of cathode-sourced PbI_2 (λ=200 nm).

nano-structure was obtained with increased washing. This result implies that the intensity of the near-band-edge emission depends on the extent of PbI_2 powder crystallinity, with increased crystallinity leading to enhanced optical properties. The observable bands are directly related to higher-order crystallinity, which is consistent with the XRD measurements. Emission band red-shift is observed in Figure 9. This could be due to increase in the particle size of PbI_2 during particle growth process. This observation is further supported by the XRD results. The broadening of PL emission

spectra is thought to be related to the increase in material crystallinity by the removal of impurities, as suggested by the SEM micrographs. Figure 10 shows the PL spectrum of cathode-sourced PbI_2 nanoparticles under 200 nm wavelength excitation, with a similar broad emission peak at around 457 nm. The optical absorption of direct band gap PbI_2 nanoparticles was estimated using the emission energy equation

$$E_g = \frac{hc}{\lambda} \tag{6}$$

where h is Planks constant, c is the speed of light and λ is a cut-off wavelength in nanometers. The optical band gap was determined by extrapolating a straight line from the peak height shown in Figure 9. The average estimated band gap E_g of both anode- and cathode-sourced PbI_2 nanoparticles was approximately 2.73 eV and 2.69 eV respectively, with $\pm$0.6 eV measurement uncertainty. The estimated band gap is in agreement with the band gap for bulk PbI_2 materials [16], [17].

5. Conclusion

Highly pure and crystalline lead (II) iodide nano-powders were successfully prepared using two separate approaches on the anode and the cathode materials obtained from a depleted SLAG accumulator. The powders exhibit good thermal stability, which is needed for the final solar cell to be stable in use over varied environmental temperatures. The crystallite size was found to be 13.703, 11.587, 12.494 and 14.320 nm. SEM micrography revealed grain-like surface morphologies with grain sizes ranging between 1.5 to 3.5 μm. Spectral PL emissions were observed in blue region from 400 to 500 nm,

attributed to the well known excitonic band. The band gap was found to be in the range of 2.69 and 2.75 eV for both methods. The present study therefore suggests effective routes and methods for the low-cost production of high quality lead (II) iodide nano-powders that have potential applications in lead iodide perovskite solar cells. The cost implications are attractive considering the abundance of discarded lead-acid accumulators.

References

[1] Zheng, Z., Liu, A., Wang, s., Li, Z., Lau, W.M., Zhang, L., 2005. *In situ growth of epitaxial lead iodide films composed of hexagonal single crystals*, Journal of Materials Chemistry, 15: 45554559, doi: 10.1039/b510077a

[2] Dmitriev, Y., Bennett, P.R., Cirignano, L.J.,Klugerman, M., Shah, K.S., 2008. *Physical modeling of the electrical properties of PbI_2 films*, Nuclear Instruments and Methods in Physics Research Section A: Accelerators, Spectrometers, Detectors and Associated Equipment, 592(3):334-345, doi:10.1016/j.nima.2008.04.003

[3] Condeles, J.F., Ando, R.A., Mulato, M., 2008. *Optical and structural properties of PbI_2 thin films*, Journal of Material Science, 43: 525-529, doi:10.1007/s10853-007-1854-9

[4] Shkir, M., Abbas, H., Siddhartha, Khan, Z.R., 2012. *Effect of thickness on the structural, optical and electrical properties of thermally evaporated PbI_2 thin films*, Journal of Physics and Chemistry of Solids, 73: 1309-1313, doi:10.1016/j.jpcs.2012.04.019

[5] Dos Santos, E.M.S., Pereira, L.S., Dements, G.J.F., 2011. *Quantum Confinement in PbI_2 Nanodisks Prepared with Cucurbit[7]uril*, Journal of the Chemical Society, 22(8): 1595-1600,

[6] Preda, V., Mihut, L., Baltog, I., Velula, T., Teodorescu, V., 2006. *Optical properties of low-dimensional PbI_2 particles embedded in polyacrylamide matrix*, Journal of Optoelectronics and Advanve materials, 8(3):909-913.

[7] Kasi, G.P., Dollahon, N.R., Ahmadi, T.S., 2007. *Fabrication and characterization of solid PbI_2 nanocrystals*, Journal of Physics D: Applied Physics, 40(6):1778

[8] Zhu, X.H., Zhao, B.J., Zhu, S,F., Jin, Y.R., He, Z.Y., Zhang, J.J., Huang, Y., 2006. *Synthesis and characterization of PbI2 polycrystals*, Crystal Research and Technology, 41(3):239-242. doi: 10.1002/crat.200510567

[9] Ma, D., Zhang, W., Zhang, M., Xi, G., Qiam, Y., 2005. *A facile hydrothermal synthesis route to single-crystalline lead iodide nanobelts and nanobelt bundles*, Journal of Nanoscience and Nanotechnology, 5(5):810-3

[10] Schiebera,M., Zamoshchik, N., Khakhana, O., Zucka, A., 2008. *Structural changes during vapor-phase deposition of polycrystalline-PbI_2 films*, Journal of Crystal Growth, 310(13):31683173, doi:10.1016/j.jcrysgro.2008.02.030

[11] Alexander, L., Klug, H.A., 1950. *Determination of Crystallite Size with*

the XRay Spectrometer, Journal of Applied Physics 21: 137-142, doi: 10.1063/1.1699612

[12] Molefe, F.V., Koao, L.F., Dejene, B,F., Swart, H.C., 2015. *Phase formation of hexagonal wurtzite ZnO through decomposition of Zn(OH)$_2$ at various growth temperatures using CBD method*, Optical Materials, 46:292-298. doi:http://dx.doi.org/10.1016/j.optmat.2015.04.034

[13] Zheng, Z., Wang, S., Li, D., Liu, A., Huang, B., Zhao, H., Zhang, L., 2007. *Morphology-controlled synthesis of lead iodine compounds from lead foils and iodine*, Journal of Crystal Growth, 308(2):398-405

[14] Derenzo, S.E., Weber, M.J., Klintenberg, M.K., 2002. *Temperature dependence of the fast, near-band-edge scintillation from CuI, HgI$_2$, PbI$_2$, ZnO:Ga and CdS:In*, Nuclear Instruments and Methods in Physics Research A, 486:214219

[15] Zhang, J., Song, T., Zhang, Z., Ding, K., Huang, F., Sun, B., 2015. *Layered ultrathin PbI2 single crystals for high sensitivity flexible photodetectors*, Journal of Material Chemistry C, 3:4402. doi: 10.1039/c4tc02712d

[16] Zhu, G., Hojamberdiev,M., Liua, P., Peng,J., Zhou, J., 2011. *The effects of synthesis parameters on the formation of PbI2 particles under DTAB-assisted hydrothermal process*, Materials Chemistry and Physics, 131:64-71.

[17] Koutselas, I., Dimos, K., Bourlinos, A., Gournis, D., Avgeropoulos, A., Agathopoulos, S., Karakassides, M.A.,2008. *Synthesis and characteriza-*

tion of PbI_2 semiconductor quantum wires within layered solids, Journal of Optoectronics and Advanced Materuals, 10(1): 58-65.